Journal of Biomedical Optics

SPIEDigitalLibrary.org/jbo

Laser speckle contrast imaging of blood flow in rat retinas using an endoscope

Adrien Ponticorvo
Damon Cardenas
Andrew K. Dunn
Daniel Ts'o
Timothy Q. Duong

SPIE

Laser speckle contrast imaging of blood flow in rat retinas using an endoscope

Adrien Ponticorvo,[a*] Damon Cardenas,[a*] Andrew K. Dunn,[b] Daniel Ts'o,[c] and Timothy Q. Duong[a,d]
[a]University of Texas Health Science Center, Research Imaging Institute, San Antonio, Texas 78229
[b]University of Texas at Austin, Department of Biomedical Engineering, Austin, Texas 78712
[c]SUNY Upstate Medical University, Departments of Neurosurgery and Neuroscience, Syracuse, New York 13210
[d]South Texas Veterans Health Care System, Department of Veterans Affairs, San Antonio, Texas 78229

Abstract. Laser speckle contrast imaging (LSCI) offers a cost-effective means to image blood flow *in vivo*. However, it is not commonly used to image rodent retinas because of the challenges associated with imaging through the curved cornea and delivering light through the highly scattering lens. A solution to overcome these problems by using LSCI in conjunction with an endoscope to obtain high spatiotemporal blood flow images is described. Its utility is demonstrated by imaging blood flow changes in rat retinas using hyperoxic, hypercapnic, and visual (flicker) stimulations. Hypercapnia increases blood flow, hyperoxia decreases blood flow, and visual stimulation increases blood flow in the retina relative to basal conditions. The time-to-peak of the LSCI response to visual stimulation is also measured. This approach may prove useful to investigate dysregulation in blood flow-evoked responses in retinal diseases and to evaluate treatment strategies in rodents. [DOI: 10.1117/1.JBO.18.9.090501]

Keywords: laser speckle imaging; retinal imaging; gas challenge; flicker stimulation.

Paper 130502LR received Jul. 16, 2013; revised manuscript received Aug. 30, 2013; accepted for publication Sep. 4, 2013; published online Sep. 24, 2013.

Blood flow in the retina can be noninvasively imaged using Doppler optical coherent tomography,[1] scanning laser-Doppler flowmetry,[2–4] laser speckle contrast imaging (LSCI),[5] and magnetic resonance imaging (MRI),[6–8] among others. LSCI, in particular, offers a cost-effective means to measure instantaneous blood flow with high-spatiotemporal resolution.[9,10] The majority of LSCI retinal applications are in humans,[11,12] with few rodent applications,[13,14] despite this, rodents are widely used for models of retinal diseases. This is in part due to the difficulties in dealing with the refractive properties of the curved cornea and the poor quality of the rodent lens, which results in challenges in delivering and receiving light to generate good images of the retina. A common approach to overcome some of these problems is to use a contact lens to be placed over the cornea.[13–15] While this approach helps to reduce refractive error, delivering coherent light to the eye remains challenging in that it requires a difficult and time-consuming alignment of the camera to find the correct angle.[14,15]

We implemented a solution to overcome these problems by using an endoscope to obtain images and to deliver light.[16,17] The optics of the endoscope help to correct the refraction of the cornea without the need for a contact lens. Additionally, the fiber-optic guide built into the endoscope is in a ring structure around the edge of the endoscope, which is very efficient in delivering uniform light to the retina without obstructing the reflected light. This same fiber-optic guide could be used to deliver laser light for generating a speckle pattern, while a camera can easily be placed on the end of the endoscope. There is also no need to align optics for the camera sensor, as the endoscope connects directly to it. We demonstrated the utility of this approach by imaging blood flow changes in the rat retina using hyperoxia, hypercapnia, and visual (flicker) stimulations.

A schematic of the imaging instrument is shown in Fig. 1(a). The animal was secured in a stereotaxis to eliminate motion, and mineral oil was placed on the surface of the cornea to prevent dryness. The endoscope (5-mm diameter, 11.5-cm length, Karl Storz 67260AA, Tuttlingen, Germany), depicted from different angles in Figs. 1(c) and 1(d), was then placed directly in contact with the mineral oil, carefully avoid pressuring the corneal surface. A laser diode (785 nm, Thorlabs, Newton, New Jersey) connected to the fiber-optic input was used to deliver light through the endoscope onto the eye using a ring-shaped illumination pattern. We would not expect the light to affect the optical properties or the physiology of the eye. The scattered laser light was captured by the CMOS camera (Basler 602f, 655×490 pixels, Basler, Ahrensburg, Germany) connected to the endoscope using a custom lens adapter (SN# OY620143-A). For green-light reflectance images, the laser diode was replaced with a green LED and delivered using a fiber-optic guide. Images from the camera were collected at a rate of 70 frames per second and an exposure time of 5 ms using custom written software. During functional activation, a slightly altered setup was used, as shown in Fig. 1(b). The 530-nm light from a green LED was combined with the laser diode output using a dual-branch light guide (Edmund Optics, Barrington, New Jersey). Figure 1(e) shows a photograph of the system in use.

All animal experiments were approved by the Institutional Animal Care and Use Committee and in accordance with the Association for Research in Vision and Ophthalmology Statement for the Use of Animals in Ophthalmic and Visual Research. Adult male Sprague-Dawley rats (~300 g, $N = 3$) were anesthetized with 1% isoflurane, paralyzed with 3.5 mg/kg pancuronium bromide to prevent eye motion,[18] and mechanically ventilated. End-tidal CO_2, heart rate, and oxygen saturation were monitored continuously and maintained within normal physiological ranges. Gas challenges were used to induce blood-flow changes in the eye. Inhalation gas was switched to either hyperoxia (100% O_2) or hypercapnia (7.5% CO_2 in air) for 5 min, and then back to breath normal air. For functional activation studies, a green LED (530 nm, Thorlabs) was used as a stimulus source and modulated at a rate of 10 Hz for 10 s.

*These authors contributed equally.

Address all correspondence to: Timothy Q. Duong, University of Texas Health Science Center, Research Imaging Institute, San Antonio, Texas 78229. Tel: 210 567 8100; Fax: 210 567 8152; E-mail: duongt@uthscsa.edu

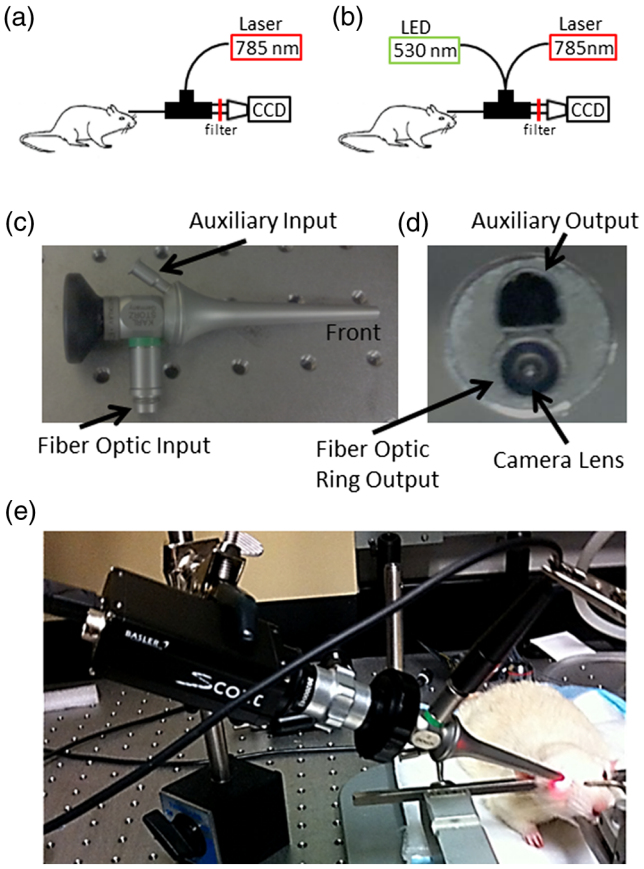

Fig. 1 Schematic of imaging setup used for (a) gas challenge experiments and (b) functional activation experiments. Side (c) and front (d) views of the endoscope used in the experiments. A photograph of the imaging system in use (e) is also shown.

The image of scattered laser light from the tissue surface, often referred to as a raw speckle image, is generated from a random static interference pattern that results from coherent light reflecting off of a rough surface. If an object consists of moving particles, as in the case with red blood cells in tissue, then the speckle pattern will fluctuate at a frequency due to the Doppler shift created by the moving particle. While other factors can affect this, these fluctuations are mainly caused by the changes in blood flow. The speckle contrast image (K) is defined as the ratio of the standard deviation (σ) to the mean intensity ($\langle I \rangle$) in a small region of the raw speckle image. Each raw speckle image was converted to a speckle contrast map in real time using optimized algorithms,[19] and each set of 10 speckle contrast images was averaged together to reduce the image-to-image variations to less than 1%. This averaged speckle contrast image was then converted to an image of relative correlation times using Eq. (1):

$$K = \frac{\sigma}{\langle I \rangle} = \sqrt{\frac{\tau}{2T}\{e^{\frac{-2T}{\tau}}\}}, \quad (1)$$

where T is the exposure time of the camera and τ is the autocorrelation time, which was estimated from the speckle contrast value. These correlation times were then used to calculate relative blood-flow changes, as the two are inversely proportional.

Green-light reflectance images were initially used to confirm the retinal vessel locations. The green-light reflectance image [Fig. 2(a)] showed the larger retinal vessels branching from the optic nerve head as well as a smaller meshwork of choroidal vasculature throughout the eye. Compared with the reflectance images, the LSCI images [Fig. 2(b)] showed better contrast of the retinal and choroidal vessels as well as relatively higher flow in the posterior ciliary artery. During the gas challenge, ocular blood flow increased from 11% to 31% during hypercapnia [Fig. 2(c)] and decreased from 23% to 40% during hyperoxia [Fig. 2(d)]. These changes are particularly apparent in the retinal vessels. There are also blood-flow changes in the "background," due to the dense vascular meshwork of the choroidal vessels. These results are consistent with blood-flow changes reported by using laser Doppler flowmetry[20] and MRI.[21]

LSCI was then used to investigate visual stimulation in the rat retina. Time-course data from several regions of interest showed increased blood flow during visual stimulation (Fig. 3). While blood flow from a given region would have signaled contributions from both the retina and the choroid, selecting regions with large identifiable retinal vessels were likely heavily weighted toward retinal blood flow.

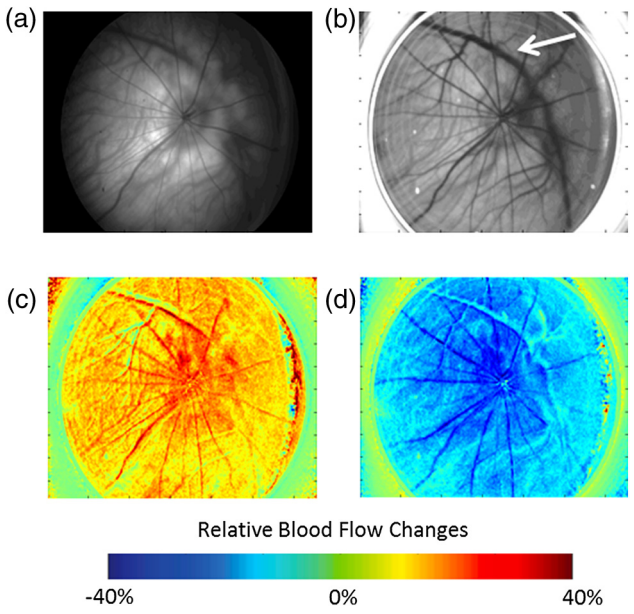

Fig. 2 (a) Green-light reflectance and (b) speckle contrast images at baseline conditions. The arrow denotes the long posterior ciliary artery. Relative blood-flow images during (c) hypercapnic and (d) hyperoxic conditions.

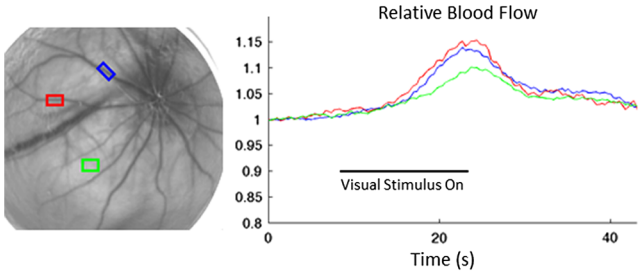

Fig. 3 During a visual stimulus experiment, regions of interest are selected in the speckle contrast image, and the time courses for those regions are shown.

The maximum blood-flow response was 10% and 15% depending on the region of interest, and the time to reach 50% of the peak blood-flow response from stimulus onset was 3.2 s in the retinal vessels, consistent with those reported previously in rats (2.25 s)[13] and humans (3.4 s).[22] Given that it is difficult to compare relative blood-flow changes across animals, the time-to-peak measurements may offer advantages in the study of retinal diseases.

While it is possible to measure hemodynamic responses by reflectance imaging, the commonly used visible light for neurological studies interferes with retinal measurement, because it stimulates the retina.[23] Moreover, the reflectance changes (which have complex signal sources) are difficult to interpret with respect to physiological parameters. By contrast, an advantage of LSCI is that it uses infrared light, which should not visually stimulate the retina,[22] and provides a single physiological parameter (ca. blood flow).

In conclusion, this study demonstrated the feasibility of performing LSCI via an endoscope to generate images of blood flow in the rat retina. Because rodents are common animal models for human retinal diseases, this approach may prove useful to investigate retinal disease pathophysiology and novel treatment strategies in rodent models. Future studies will focus on integrating interleaving LSCI and oximetric acquisition, applying this approach to study retinal diseases, and evaluating novel treatments.

Acknowledgments

This work was supported in part by the Department of Veterans Affairs (VA MERIT Award) and NIH (R01 EY018855 and R01 EY014211).

References

1. O. Tan et al., "Doppler optical coherence tomography of retinal circulation," *J. Visualized Exp.* (67), e3524 (2012).
2. G. T. Feke, "Laser Doppler instrumentation for the measurement of retinal blood flow: theory, and practice," *Bull. Soc. Belge Ophtalmol.* (302), 171–184 (2006).
3. C. E. Riva "Sub-foveal choroidal blood flow by LDF: measurement and application to the physiology and pathology of the choroidal circulation," *Bull. Soc. Belge Ophtalmol.* (302), 185–194 (2006).
4. C. E. Riva and B. Falsini, "Functional laser Doppler flowmetry of the optic nerve: physiological aspects, and clinical applications," *Prog. Brain Res.* **173**, 149–163 (2008).
5. J. D. Briers and A. F. Fercher, "Retinal blood-flow visualization by means of laser speckle photography," *Invest. Ophthalmol. Visual Sci.* **22**(2), 255–259 (1982).
6. Y. Li, H. Cheng, and T. Q. Duong, "Blood-flow magnetic resonance imaging of the retina," *Neuroimage* **39**(4), 1744–1751 (2008).
7. E. R. Muir and T. Q. Duong, "MRI of retinal and choroid blood flow with laminar resolution," *NMR Biomed.* **24**(2), 216–223 (2011).
8. Q. Peng et al., "MRI of blood flow of the human retina," *Magn. Reson. Med.* **65**(6), 1768–1775 (2011).
9. D. A. Boas and A. K. Dunn, "Laser speckle contrast imaging in biomedical optics," *J. Biomed. Opt.* **15**(1), 011109 (2010).
10. A. K. Dunn et al., "Dynamic imaging of cerebral blood flow using laser speckle," *J. Cereb. Blood Flow Metab.* **21**(3), 195–201 (2001).
11. T. Sugiyama et al., "Use of laser speckle flowgraphy in ocular blood flow research," *Acta Ophthalmol.* **88**(11), 723–729 (2010).
12. G. Watanabe, H. Fujii, and S. Kishi, "Imaging of choroidal hemodynamics in eyes with polypoidal choroidal vasculopathy using laser speckle phenomenon," *Jpn. J. Ophthalmol.* **52**(3), 175–181 (2008).
13. A. I. Srienc, Z. L. Kurth-Nelson, and E. A. Newman, "Imaging retinal blood flow with laser speckle flowmetry," *Front. Neuroenergetics* **2**(128) (2010).
14. H. Cheng, Y. Yan, and T. Q. Duong, "Temporal statistical analysis of laser speckle images and its application to retinal blood-flow imaging," *Opt. Express* **16**(14), 10214–10219 (2008).
15. H. Cheng and T. Q. Duong, "Simplified laser-speckle-imaging analysis method and its application to retinal blood flow imaging," *Opt. Lett.* **32**(15), 2188–2190 (2007).
16. J. L. Guyomard et al., "A low-cost and simple imaging technique of the anterior and posterior segments: eye fundus, ciliary bodies, iridocorneal angle," *Investig. Ophthalmol. Visual Sci.* **49**(11), 5168–5174 (2008).
17. M. Paques et al., "Panretinal, high-resolution color photography of the mouse fundus," *Investig. Ophthalmol. Visual Sci.* **48**(6), 2769–2774 (2007).
18. G. Nair et al., "Effects of common anesthetics on eye movement and electroretinogram," *Adv. Ophthalmol.* **122**(3), 163–176 (2011).
19. W. J. Tom, A. Ponticorvo, and A. K. Dunn, "Efficient processing of laser speckle contrast images," *IEEE Trans. Med. Imaging* **27**(12), 1728–1738 (2008).
20. C. E. Riva, C. J. Pournaras, and M. Tsacopoulos, "Regulation of local oxygen tension and blood flow in the inner retina during hyperoxia," *J. Appl. Physiol.* **61**(2), 592–598 (1986).
21. Y. Li, H. Cheng, and T. Q. Duong, "Blood-flow magnetic resonance imaging of the retina," *NeuroImage* **39**(4), 1744–1751 (2008).
22. C. E. Riva, E. Logean, and B. Falsini, "Visually evoked hemodynamical response and assessment of neurovascular coupling in the optic nerve and retina," *Prog. Ret. Eye Res.* **24**(2), 183–215 (2005).
23. J. Schallek and D. Ts'o, "Blood contrast agents enhance intrinsic signals in the retina: evidence for an underlying blood volume component," *Investig. Ophthalmol. Visual Sci.* **52**(3), 1325–1335 (2011).